THE JOURNAL OF BIOLOGICAL CHEMISTRY VOL. 281, NO. 19, pp. 13566–13573, May 12, 2006

p53 Is Cleaved by Caspases Generating Fragments Localizing to Mitochondria*

Received for publication, November 21, 2005, and in revised form, February 27, 2006 Published, JBC Papers in Press, March 10, 2006, DOI 10.1074/jbc.M512467200

Berna S. Sayan[1], A. Emre Sayan[1], Richard A. Knight, Gerry Melino[2], and Gerald M. Cohen

From the Medical Research Council (MRC) Toxicology Unit, Leicester LE1 9HN, United Kingdom

The p53 tumor suppressor protein exerts most of its anti-tumorigenic activity by transcriptionally activating several pro-apoptotic genes. Accumulating evidence also suggests a transcription-independent function of p53 during apoptosis. It has recently been shown that, when activated, a fraction of p53 translocates to mitochondria, causing cytochrome *c* release. We now demonstrate a caspase-dependent cleavage of p53 resulting in the generation of four fragments, two of which lack a nuclear localization signal and consequently localize to cytosol. Moreover, these two fragments translocate to mitochondria and induce mitochondrial membrane depolarization in the absence of transcriptional activity. This novel feature of p53 supports the model whereby cytosolic p53 exerts major functions in apoptosis and also suggests the presence of a positive feedback loop in which activated caspases cleave p53 to augment mitochondrial membrane depolarization.

TP53 is the most frequently mutated and intensely studied tumor suppressor gene (1, 2). After DNA damage or proto-oncogene activation, p53 is stabilized by post-translational modifications and exerts its anti-tumorigenic activity by inducing cell cycle arrest or apoptosis (3, 4). Although most data suggest that the activities of p53 are due to its sequence-specific transcription activation, there is growing but still controversial evidence that p53 exerts pro-apoptotic activity in a transcription-independent manner (5). Recently, it has been demonstrated that at the onset of apoptosis, following hypoxia or DNA damage, a small fraction of p53 translocates to mitochondria, where it interacts with Bak, Bcl-$_{XL}$, or Bcl-2 and induces cytochrome *c* release (6, 7). Cytosolic p53 was also shown to induce cytochrome *c* release by acting in a manner similar to the BH3-only pro-apoptotic proteins (8).

Due to its multifunctional nature and central role in many cellular events, p53 is a target of many post-translational regulations, such as phosphorylation, ubiquitylation, and acetylation (9). Calpains target p53 for cleavage and modify its stability (10, 11). Recently, the *p53* gene was shown to contain an alternative promoter, producing N-terminally truncated protein, and p53 translation can also start from an internal start codon, producing p47 (12). Moreover, p53 transcripts are also subjected to alternative splicing at their 3′ end (13). Thus, the *p53* gene can produce many proteins as a result of post-transcriptional and post-translational modifications, some yet to be characterized.

More than 280 proteins have been identified as caspase substrates (14). Although several structural and regulatory proteins are inactivated by caspases, others are activated to regulate key events in cell death (15–18). Substrate cleavage by caspases has also been demonstrated during cell cycle regulation and cellular differentiation (19, 20). However, cleavage of many caspase substrates is probably due to a bystander effect without any apparent biological significance.

Although most laboratories report p53 as exclusively nuclear, others ascribe a cytoplasmic function for p53. Since we observed low molecular weight p53-derived proteins following induction of apoptosis, we asked whether p53 could be processed by caspases and whether any of these cleavage products could have an effect on mitochondria.

In this study, we have demonstrated that p53 is a caspase target. Processing of p53 by caspases results in the generation of four fragments, two of which lack a nuclear localization signal and localize to mitochondria. These mitochondrial p53 fragments induce mitochondrial membrane depolarization in the absence of transcriptional activity.

EXPERIMENTAL PROCEDURES

Cell Culture and Drug Treatments—Cell lines were grown as suggested by ATCC. Transfections were carried out by using Lipofectamine 2000 reagent (Invitrogen). Apoptosis was assessed by flow cytometry using annexin V-propidium iodide staining (Bender MedSystems). Cells were treated with etoposide (35–100 μM), cisplatin (50 μM), doxorubicin (0.5 μM), or tumor necrosis factor-related apoptosis-inducing ligand (TRAIL,[3] 200 ng/ml) for induction of apoptosis. Pan-caspase inhibitor Z-Val-Ala-DL-Asp(OMe)-fluoromethyl ketone (z-VAD-fmk, Bio-Mol) was freshly added to the growth medium 1 h prior to treatment. Staurosporine (100 nM for 6 h) was used as a positive control for induction of apoptosis.

Plasmids and Luciferase Assay—Human wild type p53 (wtp53) encoding pcDNA3.1 plasmid with an N-terminal influenza hemagglutinin epitope tag was used to generate non-cleavable p53 mutants or different p53 fragments. The Stratagene QuikChange site-directed mutagenesis kit was used to mutate candidate aspartate residues to identify the caspase-cleavage site, to generate the naturally occurring p53 mutants, R248W, R249S, and the D186A non-cleavable mutants of these naturally occurring mutants. Different p53 fragments were cloned in pcDNA3.1 in-frame with green fluorescent protein, FLAG, and/or paramyxovirus of simian virus 5 (V5)-His tag using a TOPO cloning kit (Invitrogen). Luciferase assays were performed following the instructions of the Promega Dual Glo (Stop and Glo) kit with Bax, MDM2, or PG13 promoters (21). Mitochondria-targeted red fluorescent protein (Mito-RFP) plasmid was kindly provided by Prof. P. Nicotera (MRC Toxicology Unit, Leicester, UK).

In Vitro Transcription-Translation of p53 and in Vitro Caspase Cleavage Assay—Wild type and alanine-substituted p53 plasmids were *in vitro*-translated and [^{35}S]methionine-labeled by the Promega TNT-T7-coupled reticulocyte lysate system following the manufacturer's

* This work was supported by a grant from the MRC. The costs of publication of this article were defrayed in part by the payment of page charges. This article must therefore be hereby marked "*advertisement*" in accordance with 18 U.S.C. Section 1734 solely to indicate this fact.

[1] Both authors contributed equally to this work.

[2] To whom correspondence should be addressed: MRC Toxicology Unit, Hodgkin Bldg., Leicester University, Lancaster Road, P. O. Box 138, Leicester, LE1 9HN, UK. E-mail: gm89@leicester.ac.uk.

[3] The abbreviations used are: TRAIL, tumor necrosis factor-related apoptosis-inducing ligand; z-VAD-fmk, Z-Val-Ala-DL-Asp (OMe)-fluoromethyl ketone; FLp53, full-length p53; wtp53, wild type p53; Mito-RFP, mitochondrial red fluorescent protein; PARP, poly(ADP-ribose) polymerase; COX II, cytochrome *c* oxidase-complex IV subunit II.

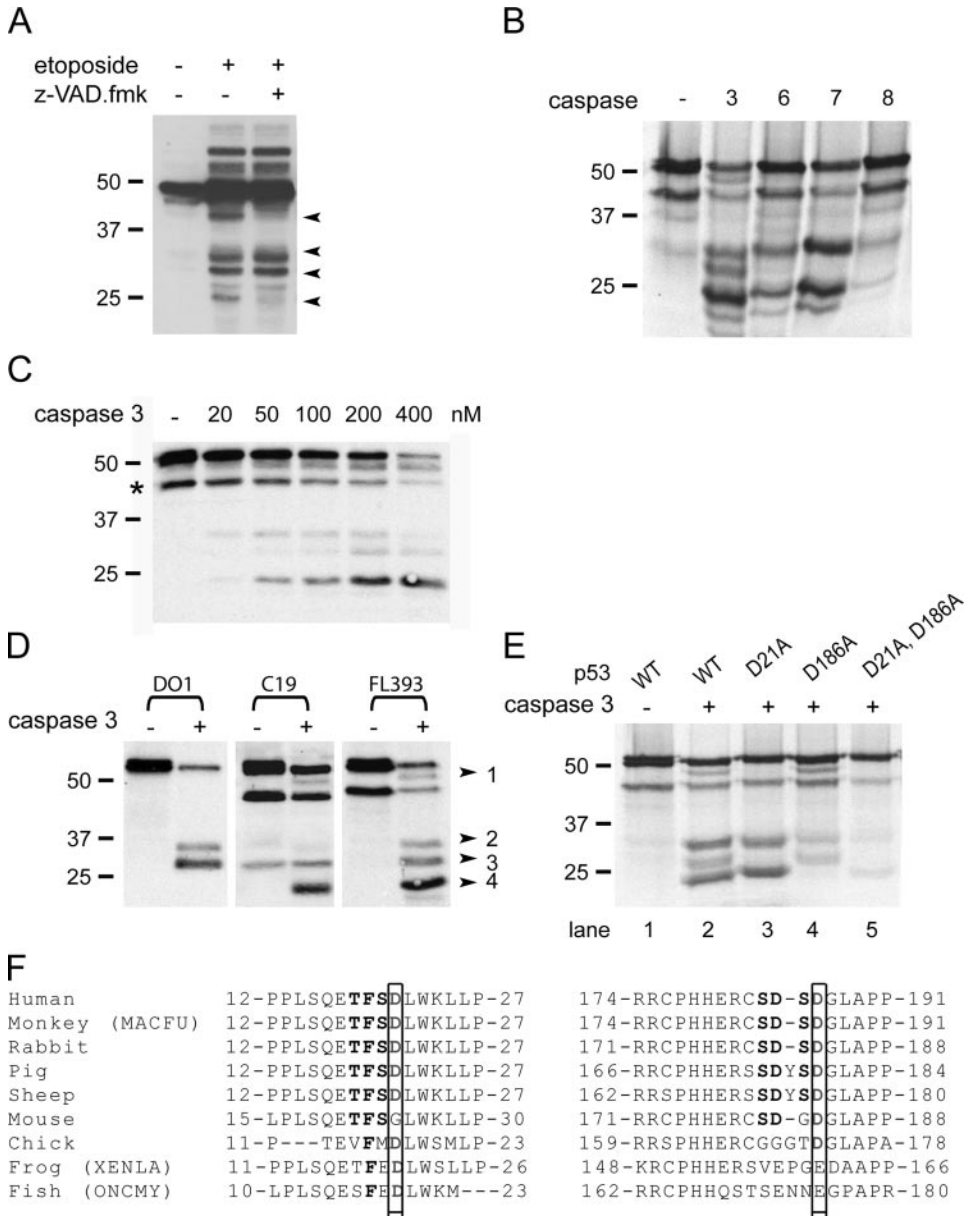

FIGURE 1. ***In vitro*-translated human p53 is cleaved by recombinant caspases.** *A,* p53 protein is modified during cellular stress yielding higher or lower molecular weight peptides. HCT116 cells were treated with etoposide (100 μM) in the presence or absence of z-VAD-fmk (100 μM) for 24 h. The *arrows* indicate several p53 forms with lower molecular weights detected by DO1-C19 antibody mixture. *B,* [^{35}S]methionine-labeled p53 protein was produced by *in vitro* transcription-translation and incubated with 200 nM recombinant active caspase-3, -6, -7, or -8 for 2 h. Caspase-6 and -7 gave an identical pattern, whereas caspase-3 cleaved p53 more extensively. *C,* p53 protein was incubated for 2 h with 20–400 nM active caspase-3. The cleavage starts with 20 nM and becomes evident by 50 nM active enzyme. The *star* indicates p53 protein lacking the N terminus, which is translated from an alternative start site (data not shown). *D,* p53 protein was subjected to Western blotting, following incubation with 200 nM recombinant active caspase-3 for 2 h. Membranes were probed with DO1, C19, or FL393 antibodies as indicated. Four major cleavage forms were detected using FL393 polyclonal antibody (indicated by *arrows* with *numbers*). *E,* p53 has two caspase-3 target sites. Two candidate caspase-3 cleavage sites, Asp^{21} and Asp^{186}, were mutated by site-directed mutagenesis. [^{35}S]Methionine-labeled *in vitro*-translated wild type (*WT*) and mutant p53 proteins were incubated with 200 nM caspase-3 for 2 h. *Lanes 1* and *2*, wild type p53; *lane 3*, D21A mutant; *lane 4*, D186A mutant; and *lane 5*, D21A,D186A double mutant. *F*, the cleavage sites are conserved among different species. Human p53 is aligned against the Swiss-Prot data base, and homology with selected species is shown. (*MACFU*, Japanese macaque; *XENLA*, African clawed frog; *ONCMY*, rainbow trout.)

instructions. For *in vitro* cleavage, proteins were incubated with either 200 nM active caspase-6, -7, or -8 or 20–400 nM recombinant active caspase-3 (18).

Antibodies and Immunoblot Analysis—For crude extracts, an equal number of cells were sonicated in 2× Laemmli buffer and boiled at 95 °C for 5 min. Mitochondria were isolated using the Pierce mitochondria isolation kit (chemical method). Actin and p53 antibodies DO1, 1801, C19, and FL393 were purchased from Santa Cruz Biotechnology. Poly (ADP-ribose) polymerase (PARP) antibody was from Alexis Biomedicals, proliferating cell nuclear antigen antibody was from BD Biosciences, and cytochrome *c* oxidase-complex IV subunit II (COX II) antibody was from Molecular Probes. The quantitation of bands was performed using NIH-Scion software.

Immunofluorescence—H1299 or SaOS-2 cells (10^5) were plated on coverslips and transfected with full-length p53 (FLp53) or p53 fragments, alone or in combination with mito-RFP. Cells were fixed with 4% paraformaldehyde in phosphate-buffered saline for 30 min. Following fixation, cells were permeabilized for 2 min in phosphate-buffered saline containing 0.1% Triton-X-100, blocked in 2.5% goat serum for 30 min, and incubated with the primary antibody for 1 h. Alexa-488-conjugated secondary antibody was used as recommended by the supplier (Molecular Probes), and the nuclei were counterstained with 4′,6-diamidino-2-phenylindole. Slides were analyzed with a confocal laser microscope (ZEISS LSM 510).

Analysis of Mitochondrial Membrane Depolarization—Following transfection of HeLa or H1299 cells with relevant plasmids, cells were trypsinized, counted, pelleted, and resuspended in fresh medium (10^6 cells/ml). After a 25-min recovery in the cell culture incubator, tetramethylrhodamine ethyl ester was added to the cells (50 ng/ml). After a further 5-min incubation, membrane potential was read using a flow cytometer (FACSCalibur, BD Biosciences).

RESULTS AND DISCUSSION

p53 Is Cleaved by Caspases—During cellular stress, p53 protein levels increase, and this is accompanied by the appearance of several lower and higher molecular weight p53-derived peptides (Fig. 1*A*). The high molecular weight p53 protein forms have been identified as ubiquitylated forms of full-length p53, whereas some of the low molecular

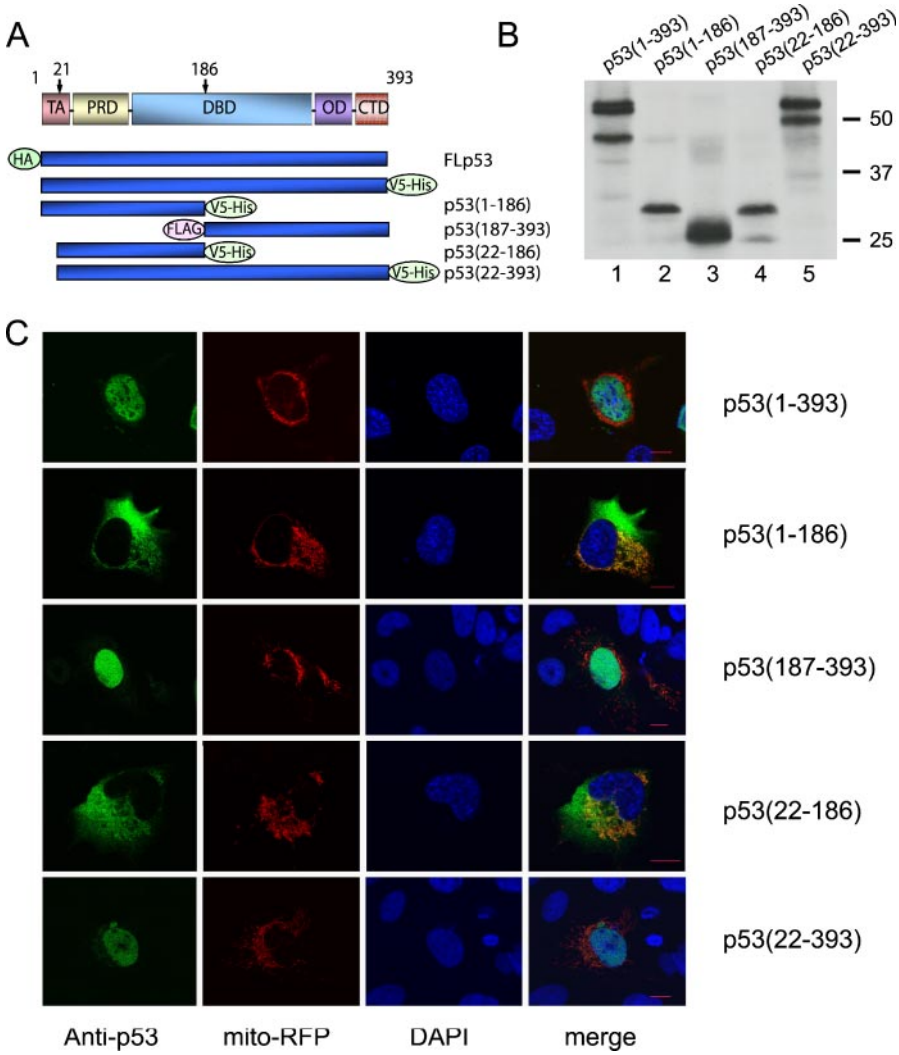

FIGURE 2. **Cellular localization of caspase-cleaved p53 fragments.** *A,* The constructs generated for this study are schematically represented with the corresponding tags. *Boxes* indicate different functional domains of p53. Since the retention of caspase recognition and cleavage sites would result in the cleavage of the C-terminal tags of fragments p53-(1–186) and p53-(22–186), these were cloned by deleting the aspartate residue of the caspase recognition site (*i.e.* p53-(1–186) was cloned as p53-(1–185) in-frame with the C-terminal tag). *TA*, transactivation domain; *PRD*, proline-rich domain; *DBD*, DNA binding domain; *OD*, oligomerization domain; *CTD*, C-terminal domain. *B,* H1299 cells were transfected with FLp53 or p53 fragments. 24 h after transfection, an equal number of cells were lysed in Laemmli buffer and subjected to Western blotting using the FL393 antibody. *Lane 1*, FLp53; *lane 2*, p53-(1–186); *lane 3*, p53-(187–393); *lane 4*, p53-(22–186); and *lane 5*, p53-(22–393). *C,* SaOS-2 cells were plated on coverslips and transfected with FLp53 or p53 fragments. 24 h after transfection, cells were fixed, permeabilized, and probed with FL393 antibody. The nucleus was stained with 4′,6-diamidino-2-phenylindole (*DAPI*), and Mito-RFP was used to localize mitochondria. FLp53 and C-terminal fragments (p53-(187–393) and p53-(22–393)) are predominantly nuclear, whereas N-terminal p53 fragments (p53-(1–186) and p53-(22–186)) are mainly localized to the cytoplasm. A portion of the cytoplasmic fragments co-localizes with mitochondria.

weight forms are derived from alternative splicing, differential promoter usage, or calpain processing (9, 10, 13).

To investigate the possibility that some of the small p53 protein fragments could be due to caspase cleavage, we incubated recombinant active caspases with *in vitro*-translated [^{35}S]methionine-labeled p53 protein. Caspase-3, -6, and -7, but not caspase-8, cleaved human p53, revealing several products (Fig. 1*B*). The cleavage pattern of these caspases was similar, although caspase-3 cleaved p53 more extensively; therefore, we focused our work on p53 cleavage by caspase-3. p53 cleavage by caspase-3 yielded four major products and was evident even with 50 nM active caspase-3 (Fig. 1*C*). These results demonstrate that different caspases can cleave p53 and that there is more than one cleavage site for caspase 3.

In silico analysis of the p53 protein sequence did not reveal any classical caspase recognition site; therefore, we aimed to locate the cleavage sites by antibody mapping. p53 cleavage products were separated by SDS-PAGE and probed with three different p53 antibodies. With the N-terminal-specific DO1 antibody, we detected two cleavage products (fragments 2 and 3, Fig. 1*D*). The C-terminal-specific C19 antibody detected only fragments 1 and 4, and the polyclonal FL393 antibody detected all four cleavage products (Fig. 1*D*). These data suggest that there are two cleavage sites, one located at the N terminus and the other located in the central portion of the protein.

Based on the molecular weights of the fragments and the results obtained by antibody mapping, we focused on two potential sequences, namely ^{18}TFSD^{21} and ^{183}SDSD^{186} (Fig. 1*E*). Wild type and D21A, D186A p53-expressing plasmids were translated in the presence of [^{35}S]methionine and incubated with caspase-3. Cleavage of the D21A mutant resulted in the formation of fragments 2 and 4, whereas only fragment 1 was produced following cleavage of the D186A mutant (Fig. 1*E*). When both Asp^{21} and Asp^{186} residues were mutated, none of the cleavage products was observed. Therefore, fragment 1 corresponds to p53-(22–393), fragment 2 corresponds to p53-(1–186), fragment 3 corresponds to p53-(22–186), and fragment 4 corresponds to p53-(187–393). The cleavage sites are conserved in higher eukaryotes from fish to human (Fig. 1*F*). Taken together, our data demonstrate the presence of two caspase-3 cleavage sites in p53, at residues Asp^{21} and Asp^{186}.

p53 Fragments Localize to Mitochondria—To evaluate whether these cleavage products possess a biological function, we generated plasmids harboring either FLp53 or the various fragments with either C- and/or N-terminal tags (Fig. 2*A*). Following transfection, all fragments were expressed (Fig. 2*B*), and marked differences were observed in their cellular localization (Fig. 2*C*). FLp53, p53-(22–393), and p53-(187–393), which contain the nuclear localization signal (22), exhibited a predominant nuclear staining. In contrast, p53-(1–186) and p53-(22–186) were mostly localized to the cytoplasm (Fig. 2*C*). Co-expression of these fragments with mito-RFP revealed that a portion of p53-(1–186) and p53-(22–186) was localized to mitochondria.

Next we asked whether these p53 fragments have an effect on mitochondria. HeLa cells were transfected with FLp53 or with the four p53

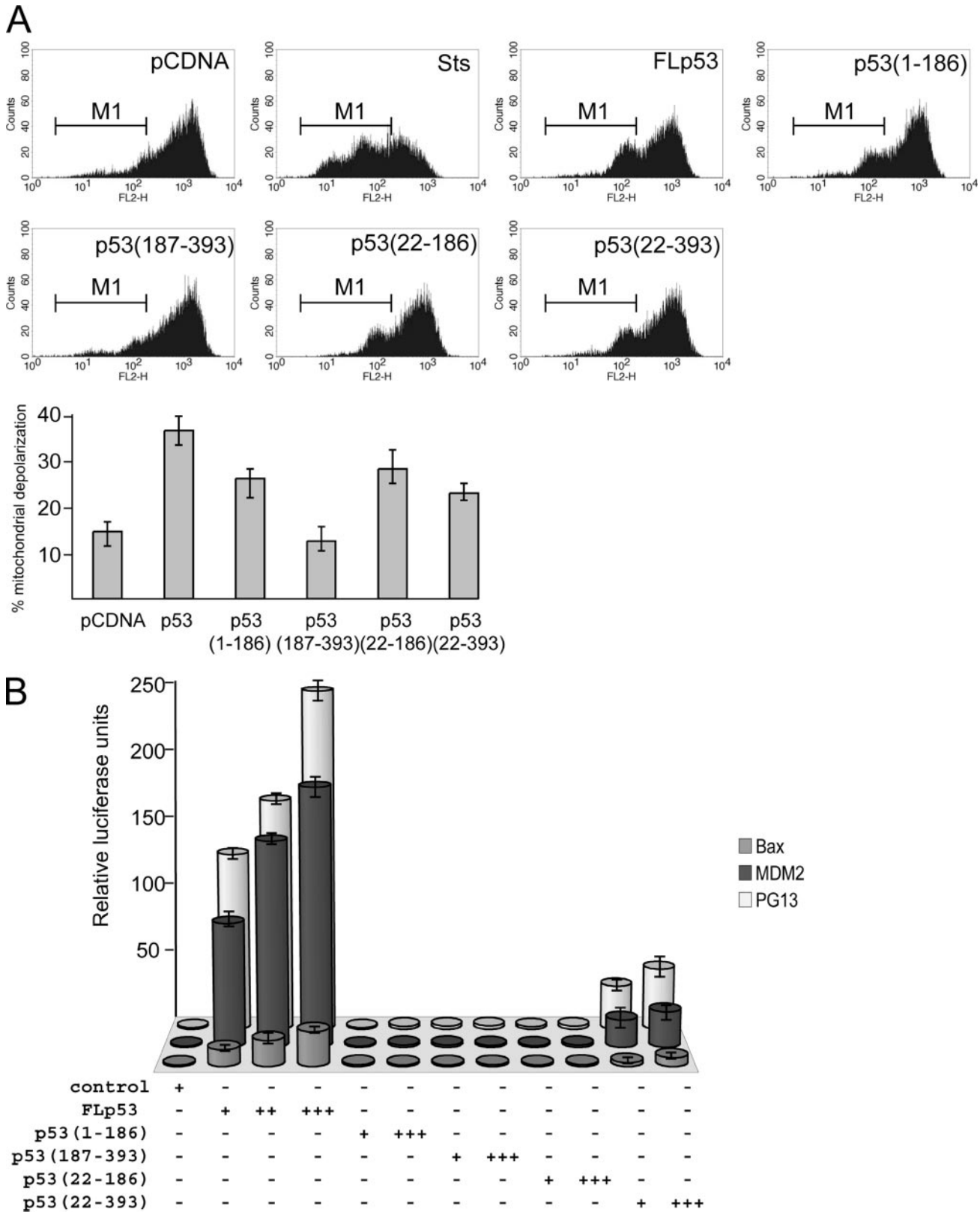

FIGURE 3. **p53 fragments induce transcription-dependent and -independent mitochondrial membrane depolarization.** *A,* HeLa cells were transfected with FLp53 and p53 fragments and processed for tetramethylrhodamine ethyl ester staining after 36 h. Staurosporine (*Sts*) (100 nM for 6 h) was used as a positive control. Apoptotic cells displayed a decreased signal in the FL2 channel. The number of cells having low FL2 signal were quantified against the whole population. p53-(187–393)-transfected cells gave similar amounts of depolarization as mock (*pCDNA*)-transfected cells (12 and 14%, respectively). FLp53 exerted the most profound effect on mitochondrial membrane potential (35%); however, the p53-(22–186) and p53-(1–186) fragments localized to the mitochondria also produced membrane depolarization. The p53 fragment, p53-(22–393), showed a 22% loss of the mitochondrial membrane potential. *B,* p53 induces the transcription from Bax, Mdm2, and PG13 promoters, whereas p53-derived fragments have no transactivation activity on their own, except for p53-(22–393), which retains a weak activity. p53 or p53 fragments were transfected in increasing concentrations as indicated by plus signs. +, 15 ng; ++, 50 ng; or +++, 100 ng of relative plasmid.

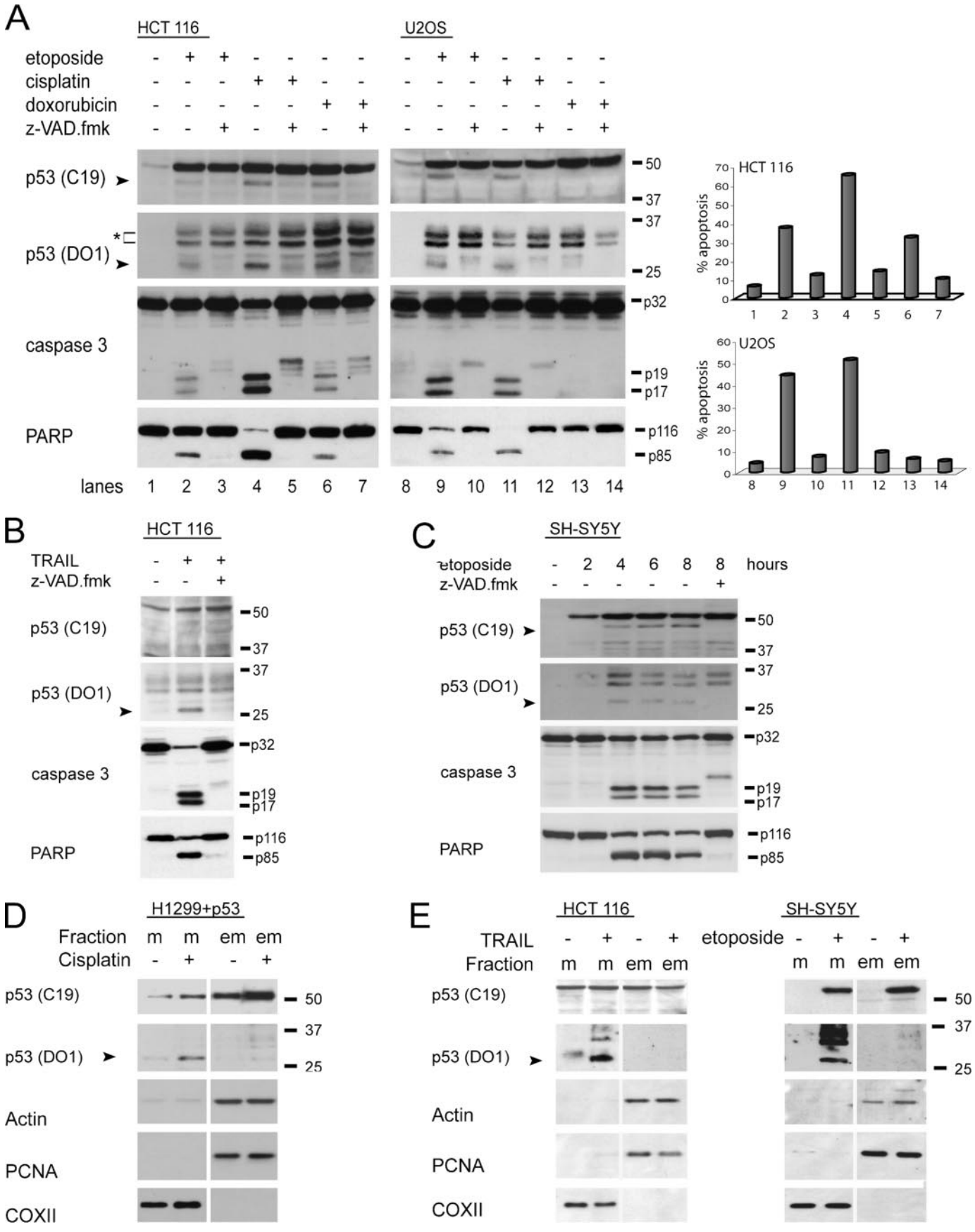

FIGURE 4. **Endogenous p53 is cleaved by caspases during apoptosis.** *A*, HCT116 and U2OS cells were treated with etoposide (75 μM), cisplatin (50 μM), or doxorubicin (0.5 μM) for 24 h in the presence or absence of z-VAD-fmk (100 μM). Apoptosis was measured by fluorescence-activated cell sorter analysis for annexin V staining. An equal number of cells were sonicated in Laemmli buffer and subjected to Western blotting for the analysis of p53 processing, caspase-3 and PARP cleavage. The *arrows* indicate two major p53 cleavage products

fragments, and mitochondrial membrane potential was analyzed by tetramethylrhodamine ethyl ester staining. 35% of cells showed mitochondrial depolarization with FLp53 (Fig. 3*A*). The nuclear p53 fragment (p53-(187–393)) and empty vector had no effect on mitochondria (14 and 12% respectively), whereas the other three p53 fragments produced a significant mitochondrial membrane depolarization. p53-(22–393) caused a 22% loss of membrane potential, whereas the fragments that were localized to mitochondria, p53-(1–186) and p53-(22–186), showed 25 and 27% mitochondrial depolarization, respectively. To rule out the possibility that mitochondrial membrane depolarization caused by p53 fragments is through transactivation, we tested the fragments on several p53 target promoters. Luciferase reporter assays with Bax, MDM2, and PG13 promoters demonstrated that p53-(1–186), p53-(22–186), and p53-(187–393) were transcriptionally inactive (Fig. 3*B*). p53-(22–393) retained a weak transcriptional activity, which may explain the mitochondrial depolarization caused by the overexpression of this fragment (Fig. 3, *A* and *B*). Thus, p53-(1–186) and p53-(22–186) cause mitochondrial membrane depolarization independent of p53-dependent transactivation.

Endogenous p53 Is Processed during DNA Damage and TRAIL-induced Apoptosis—We induced apoptosis in HCT116 and U2OS cells by TRAIL or DNA-damaging agents such as etoposide, cisplatin, or doxorubicin to demonstrate the presence of endogenous p53 caspase-cleavage products. In both cell lines, DNA-damaging agents induced apoptosis, as assessed by phosphatidylserine externalization, processing of caspase-3, and PARP cleavage (Fig. 4*A*, *lanes 2*, *4*, *6*, *9*, and *11*). Apoptosis induced by these agents was associated with the appearance of two p53-related fragments. The C-terminal-specific C19 antibody detected a fragment of ~45 kDa, corresponding to p53-(22–393), whereas the DO1 antibody detected a fragment of ~25 kDa, corresponding to p53-(1–186) (Fig. 4*A*). Generation of these cleavage products was caspase-dependent as it was blocked with z-VAD-fmk (Fig. 4*A*, *lanes 3*, *5*, *7*, *10*, and *12*). Although we detected all of the four fragments *in vitro*, we could not detect p53-(22–186) and p53-(187–393) with any of the p53 antibodies used (DO1, 1801, FL393, and C19) *in vivo*. Each of these agents also induced the formation of several other p53 forms/fragments, which were not inhibited by z-VAD-fmk (Fig. 4*A*, indicated by *star*), suggesting the caspase-independent formation of these products. Caspase-dependent p53 processing was also observed in HCT116 cells when apoptosis was induced by TRAIL (Fig. 4*B*). However, only the small (p53-(1–186)) fragment was detected. The failure to observe p53-(22–393) may be due to the rapid progression of apoptosis by TRAIL, which, in contrast to DNA-damaging agents, does not result in p53 accumulation. To evaluate the *in vivo* kinetics of p53 cleavage, SH-SY5Y cells were treated with etoposide (Fig. 4*C*). Caspase-dependent cleavage of p53 was detected as early as 4 h and was associated with the appearance of processed caspase-3 and cleaved PARP. Treatment with z-VAD-fmk abolished the processing of p53. These results demonstrate that a fraction of endogenous p53 protein is cleaved by caspases during apoptosis induced either by the intrinsic or by the extrinsic pathways.

To verify that the N-terminal p53 fragment detected by the DO1 antibody in cells (Fig. 4, *A–C*) is the mitochondrial p53 fragment (p53-(1–186)), we transfected H1299 cells with FLp53 and treated them with cisplatin. Lysates from isolated mitochondria were subjected to Western blotting. The fragment corresponding to p53-(1–186) was detected mostly in the mitochondrial fraction (Fig. 4*D*). Purity of the subcellular fractions was assessed by actin, proliferating cell nuclear antigen, and COX II Western blots. We could not detect the p53-(22–393) fragment in either of the fractions by using the C19 antibody. The kit we used was exclusively for mitochondria isolation (Pierce mitochondria isolation kit). Therefore, we believe that this p53 fragment was lost during the mitochondrial purification procedure. After having detected the caspase-generated p53 fragment in mitochondria by overexpression of FLp53, we wanted to verify the presence of the mitochondrial p53 fragment in cells harboring endogenous wild type p53 following caspase activation. Apoptosis was induced by TRAIL or etoposide treatment in HCT116 and SH-SY5Y cells, respectively, and assessed by caspase-3 processing and PARP cleavage, using non-fractionated lysates (data not shown). Supporting our overexpression data, we observed the endogenous fragment corresponding to p53-(1–186) predominantly in the mitochondrial fraction (Fig. 4*E*). This suggests that the p53-(1–186) detected in cells undergoing apoptosis is mostly mitochondrial and that this fragment localizes to mitochondria independent of the induction pathway of apoptosis, *i.e.* by activation of the extrinsic or the intrinsic pathway. Therefore, by using different drugs in cell lines of different origin, we observed the same effect, providing evidence to support the generality of this phenomenon that cleavage of p53 and localization of the cleavage product to mitochondria is a common occurrence.

Our results suggest that although most of the apoptotic activity of p53 relies on its transcription activity, p53 protein can contribute to the apoptotic process directly following caspase activation. To ascertain the approximate contribution of caspase cleavage-dependent activities of p53 to apoptosis, we compared the apoptotic activities of wtp53, D21A, and D186A non-cleavable mutants. As our initial experiments showed that the non-cleavable mutants are potentially more apoptotic than wtp53 (data not shown), we analyzed the transcriptional activities of these mutants. We observed that both of the non-cleavable mutants are transcriptionally active on the Bax and MDM2 promoters (Fig. 5*A*). Also, our attempts to generate stable cell lines expressing these mutants yielded very few colonies as compared with wtp53, with no protein expression from any (0 colonies for D186A and D21A, as compared with 10 colonies expressing wtp53, data not shown). Interestingly, most naturally occurring mutations inhibit the transcriptional activity of p53, whereas artificially mutating p53 in residues other than the ones observed in tumors may even result in an enhanced transcriptional activity (23). In parallel with these observations, we found that Asp^{21} and Asp^{186} mutations are represented very rarely (less than 12 times among 14,000 p53 mutations) in the International Agency for Research on Cancer p53 tumor mutation data base (24).

detected by the C19 and DO1 antibodies, which were abrogated in the presence of z-VAD-fmk. The *star* indicates two caspase-independent p53-derived peptides. Graphs demonstrate percent apoptosis in HCT116 and U2OS cells. Each column represents the corresponding lane. *B,* death receptor-mediated apoptosis was induced by incubating HCT116 cells with TRAIL (200 ng/ml) for 8 h, with or without z-VAD-fmk (20 μM). Since p53 accumulation was not observed during TRAIL-mediated apoptosis, three times more protein was loaded as compared with drug-induced apoptosis. p53 cleavage was assessed using C19 and DO1 antibodies. Note that only the mitochondrial p53 fragment is present in TRAIL-treated HCT116 cells. *C,* SH-SY5Y cells were incubated with etoposide (35 μM) for 2, 4, 6, and 8 h with or without z-VAD-fmk (100 μM). p53 processing starts as early as 4 h in these cells, being concurrent with the activation of caspase-3 and cleavage of PARP. *D,* mitochondrial (*m*) localization of p53-(1–186) following DNA damage in H1299 cells overexpressing FLp53. H1299 cells were transfected with FLp53. 12 h after transfection, cells were treated with cisplatin (50 μM) for 24 h. Cells were harvested, and mitochondria were isolated using the Pierce mitochondria isolation kit. C19 and DO1 antibodies were used to detect p53 in the mitochondrial and extra-mitochondrial (*em*) fractions. Using the C19 antibody, we could not detect the p53-(22–393) fragment in either of the fractions. The procedure we used involves several centrifugation steps with some precipitates being discarded. It is possible that this p53 fragment was lost during mitochondrial purification. The *arrow* indicates the p53-(1–186) fragment, which is predominantly in the mitochondrial fraction. COX II, actin, and proliferating cell nuclear antigen (*PCNA*) were used as mitochondrial, cytoplasmic, and nuclear markers, respectively. *E,* mitochondrial localization of p53-(1–186) following induction of apoptosis in cells harboring wtp53. Apoptosis was induced in HCT116 cells by TRAIL and by etoposide treatment in SH-SY5Y cells. 80 μg of protein from each fraction was subjected to Western blotting to detect mitochondrial p53 fragment p53-(1–186).

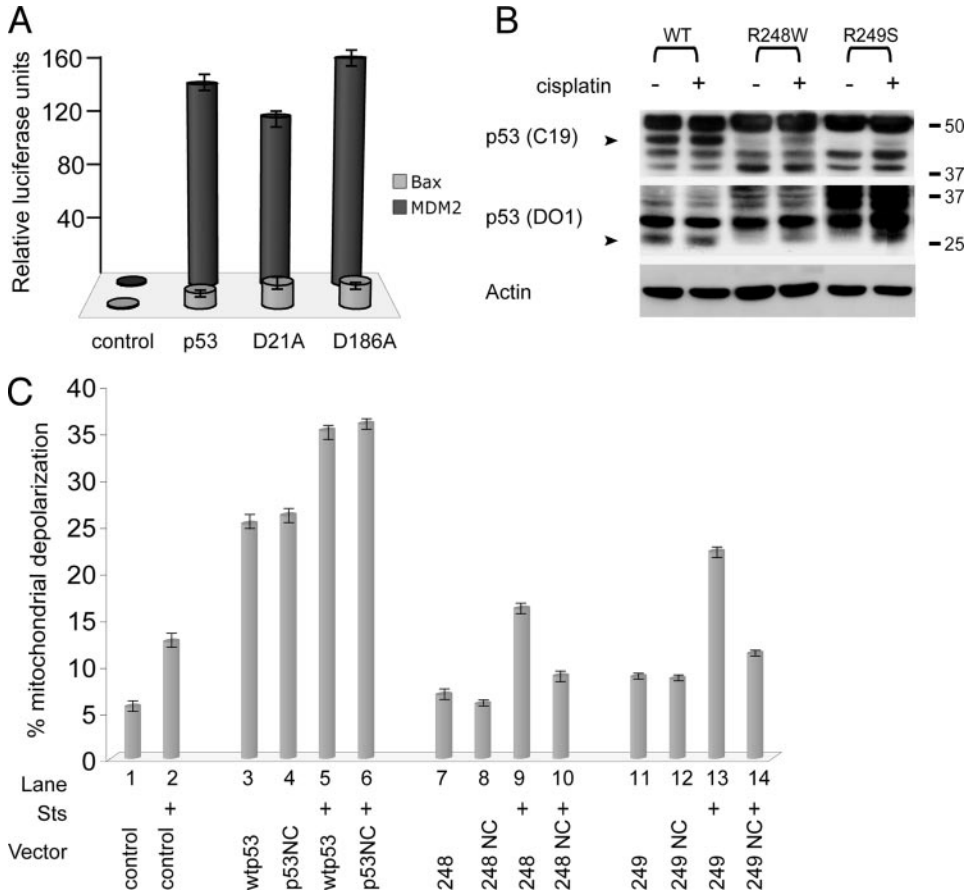

FIGURE 5. **Functional characterization of non-cleavable p53.** *A*, the transcription activity of wtp53, D186A, and D21A was assayed on Bax and MDM2 promoters. The non-cleavable mutants were more active then wtp53 on Bax promoter and comparable activity on MDM2 promoter. *B*, mutant p53 can be cleaved by caspases. Two naturally occurring mutants of p53 and wtp53 were overexpressed in H1299 cells. Both mutant p53 proteins were cleaved following an apoptotic stimulus. The cleavage of wtp53 was more extensive than that of the mutants with or without apoptotic stimuli, probably because wtp53 is inducing apoptosis without requiring any other stimulus. *WT*, wild type. *C*, mutant p53 induces more mitochondrial membrane depolarization as compared with non-cleavable mutant p53 when apoptosis is induced by staurosporine (*Sts*) as described in the legend for Fig. 3. Apoptosis was induced after 36 h, and the cells were processed 6 h after induction of apoptosis. H1299 cells were transfected with wtp53, 248 (p53(R248W)), 249 (p53(R249S)), or the non-cleavable (*NC*) mutants of these plasmids. The difference between mutant p53 and control (*pCDNA*) shows the contribution of mutant p53 to apoptosis (compare *lanes 1* and *2* with *lanes 7*, *9* and *11*, and *13*), whereas the difference between mutant p53 and non-cleavable mutant p53 shows the contribution of the caspase processing to apoptosis (compare *lanes 9* and *10* and with *lanes 13* and *14*).

To characterize the importance of p53 cleavage on apoptosis as well as excluding any transcriptional activity, we used naturally occurring p53 mutants. 10% of all p53 mutations are at codons 248 (R → (W/Q)) and 249 (R → S), resulting in the formation of transcription-deficient p53. Therefore, we generated p53 plasmids with these codon substitutions, with or without D186A. We expressed these p53 plasmids in p53-null H1299 cells and induced apoptosis with cisplatin. Although the p53 mutants were cleaved (Fig. 5*B*), none of the D186A mutants were processed (data not shown). As the D186A mutant is transcriptionally active (Fig. 5*A*), we assayed the transcriptional activities of these mutants and their non-cleavable derivatives. We observed that all of them are transcriptionally inactive (data not shown).

To demonstrate the impact of caspase cleavage of p53 on apoptosis, we overexpressed wtp53, naturally occurring p53 mutants, and non-cleavable naturally occurring p53 mutants in H1299 cells. 36 h after transfection, we treated cells with staurosporine (100 nM) for 6 h and analyzed the cells for mitochondrial membrane depolarization. We observed that mutant p53 induces a greater loss in mitochondrial membrane potential than the non-cleavable counterpart following induction of apoptosis (Fig. 5*C*). Wtp53 was clearly more potent at inducing mitochondrial membrane depolarization in the presence or absence of an apoptotic stimulus than any of the mutants (Fig. 5*C*). Our observations provide evidence that the apoptotic function of p53 is mostly transcription-dependent, but there is also a small but significant proportion that is transcription-independent and acquired after caspase activation, possibly to promote cells toward the point of no return.

Our results suggest that following caspase activation, p53 gains a transcription-independent function to reinforce apoptosis. This may lead to the formation of a positive feedback loop in which p53 accumulation induces caspase activation, resulting in p53 cleavage and promotion of apoptosis. Moreover, mutant p53 proteins that are observed in more than 50% of all tumors can also be targets of caspases, suggesting that they may still be able to induce mitochondrial depolarization, attributing a wild type p53 function to mutant p53.

Acknowledgments—We thank Dr. Xiao-Ming Sun for the active caspases, Dr. Nick Harper for TRAIL, and Drs. M. Rossi and M. J. Pinkoski for critical reading of the manuscript.

REFERENCES

1. Hollstein, M., Sidransky, D., Vogelstein, B., and Harris, C. C. (1991) *Science* **253,** 49–53
2. Vousden, K. H., and Prives, C. (2005) *Cell* **120,** 7–10
3. Vousden, K. H., and Lu, X. (2002) *Nat. Rev. Cancer* **2,** 594–604
4. Oren, M. (2003) *Cell Death Differ.* **10,** 431–442
5. Chipuk, J. E., and Green, D. R. (2003) *J. Clin. Immunol.* **23,** 355–361
6. Leu, J. I., Dumont, P., Hafey, M., Murphy, M. E., and George, D. L. (2004) *Nat. Cell Biol.* **6,** 443–450
7. Mihara, M., Erster, S., Zaika, A., Petrenko, O., Chittenden, T., Pancoska, P., and Moll, U. M. (2003) *Mol. Cell* **11,** 577–590
8. Chipuk, J. E., Kuwana, T., Bouchier-Hayes, L., Droin, N. M., Newmeyer, D. D., Schuler, M., and Green, D. R. (2004) *Science* **303,** 1010–1014
9. Brooks, C. L., and Gu, W. (2003) *Curr. Opin. Cell Biol.* **15,** 164–171
10. Kubbutat, M. H., and Vousden, K. H. (1997) *Mol. Cell. Biol.* **17,** 460–468
11. Pariat, M., Carillo, S., Molinari, M., Salvat, C., Debussche, L., Bracco, L., Milner, J., and Piechaczyk, M. (1997) *Mol. Cell. Biol.* **17,** 2806–2815
12. Courtois, S., Verhaegh, G., North, S., Luciani, M. G., Lassus, P., Hibner, U., Oren, M., and Hainaut, P. (2002) *Oncogene* **21,** 6722–6728
13. Bourdon, J. C., Fernandes, K., Murray-Zmijewski, F., Liu, G., Diot, A., Xirodimas, D. P., Saville, M. K., and Lane, D. P. (2005) *Genes Dev.* **19,** 2122–2137
14. Fischer, U., Janicke, R. U., and Schulze-Osthoff, K. (2003) *Cell Death Differ.* **10,** 76–100
15. Li, H., Zhu, H., Xu, C. J., and Yuan, J. (1998) *Cell* **94,** 491–501
16. Ricci, J. E., Munoz-Pinedo, C., Fitzgerald, P., Bailly-Maitre, B., Perkins, G. A.,

Yadava, N., Scheffler, I. E., Ellisman, M. H., and Green, D. R. (2004) *Cell* **117,** 773–786
17. Sakahira, H., Enari, M., and Nagata, S. (1998) *Nature* **391,** 96–99
18. Sun, X. M., Butterworth, M., MacFarlane, M., Dubiel, W., Ciechanover, A., and Cohen, G. M. (2004) *Mol. Cell* **14,** 81–93
19. Arama, E., Agapite, J., and Steller, H. (2003) *Dev. Cell* **4,** 687–697
20. Kennedy, N. J., Kataoka, T., Tschopp, J., and Budd, R. C. (1999) *J. Exp. Med.* **190,** 1891–1896
21. Blagosklonny, M. V., Giannakakou, P., Romanova, L. Y., Ryan, K. M., Vousden, K. H., and Fojo, T. (2001) *Carcinogenesis* **22,** 861–867
22. Addison, C., Jenkins, J. R., and Sturzbecher, H. W. (1990) *Oncogene* **5,** 423–426
23. Kakudo, Y., Shibata, H., Otsuka, K., Kato, S., and Ishioka, C. (2005) *Cancer Res.* **65,** 2108–2114
24. Soussi, T., Dehouche, K., and Beroud, C. (2000) *Hum. Mutat.* **15,** 105–113